

CONCEPTUAL DESIGN OF THE ESS-SCANDINAVIA

S.Peggs (ESSS/BNL), R.Calaga (BNL), R.Duperrier (CEA-Saclay), J. Stovall (CERN), M.Eshraqi & F.Plewinski (ESSS), M.Lindroos & G.Papotti (ESSS/CERN), A. Jansson (FNAL).

Abstract

The conceptual design of the long pulse 5 MW ESSS spallation neutron source draws heavily on state-of-the-art mature technologies, incorporating advances with spoke resonator cavities. Potential upgrades may increase the average beam power to 7.5 MW.

OVERVIEW

Proton beam macro-pulses around 1.0 ms are close to ideal from the **users point of view**[1]. Pulse repetition rates as large as 33 Hz are viable, although rates of 20 Hz or less are preferred. The 22 neutron instruments must be served with very high reliability. Currently the PSI SINQ cyclotron achieves $\sim 90\%$ reliability, while the more complex SNS SRF linac achieves $\sim 80\%$ at 680 kW. Reliability is related to maintainability, so the ESS requires low beam loss rates (preferably $\ll 1$ W/m with localized exceptions) to control beam component activation. Reliability and low losses run counter to the desire for high performance, low cost, and low risk in construction and commissioning.

Table 1: Primary ESSS performance parameters in the long pulse conceptual design. There is no accumulator ring.

INPUT		Nominal	Upgrade
Average beam power	[MW]	5.0	7.5
Macro-pulse length	[ms]	2.0	2.0
Pulse repetition rate	[Hz]	20	20
Proton kinetic energy	[GeV]	2.5	2.5
Peak coupler power	[MW]	1.0	1.0
Beam loss rate	[W/m]	< 1.0	< 1.0
OUTPUT			
Duty factor		0.04	0.04
Ave. pulse current	[mA]	50	75
Ion source current	[mA]	60	90
Total linac length	[m]	418	418

The **primary parameters** in Tab. 1 evolved from the values originally proposed in 2003, with almost the same linac components[2]. The most significant changes are the current decrease (150 mA to 60 mA) and the energy increase (1.0 GeV to 2.5 GeV). The **beam energy** is increased while keeping the overall length almost constant by raising the SC elliptical cavity gradient. The neutron flux is almost unchanged – the number of neutrons per proton-Joule is almost constant above 1 GeV. The final focusing system is modified. An active beam painting scheme is being considered. The **average beam current** reduction, enabled

mainly by the increased beam energy, in turn reduces the space charge forces and so helps to minimize halo generation at low energies, where the beam quality for the whole linac is defined. Lowering the beam current eliminates the need for a beam funnel to combine beams from two front-ends. Beam funnels have never been used in routine accelerator operations, although proof-of-principle experiments have been successful. Lower beam currents reduce the commissioning time, reduce beam losses, and facilitate an upgrade to higher beam powers. The maximum **cavity gradient** in the high current SRF linac is limited by the maximum peak power that can be fed via the **power couplers**. Current technologies limit the peak coupler power to about 1.0 MW/m, sufficient for a peak gradient of 15 MV/m in a 5-cell 704 MHz cavity accelerating a 60 mA beam. This is consistent with present technology. Increasing the **repetition rate** slightly from 16.67 Hz to 20 Hz is acceptable to the user community and helps keep the average current low. It also avoids possible problems related to subharmonics at 1/3 of the power grid frequency.

Upgrade options include: 1) Increasing the current to 90 mA with all other parameters constant, delivering **7.5 MW long pulses**; 2) Adding an accumulator ring to provide **2.5 MW short pulses** to a second target station, in addition to 5 MW long pulses; 3) Doubling the rate to 40 Hz, filling 3 out of 4 buckets, with **2.5 and 5 MW long pulses** at 10 and 20 Hz to 2 target stations.

RADIO FREQUENCY SYSTEMS

Linac sub-systems are summarized in Fig. 1 and Tab. 2. A single ECR proton **ion source** generates 60 mA, 2 ms pulses[3, 4]. Such sources have demonstrated routine operation with currents > 100 mA, with $> 99\%$ reliability. The beam pulse rise time of 1 to 2 ms is reduced to ~ 100 ns using a chopper included in the extraction system by segmenting one electrode. The **LEBT** line matches the beam extracted from the ion source into the RFQ with minimal emittance growth, using a dual solenoid system. Magnetic focusing permits space charge neutralization via the ionization of the residual gas. The slow chopper system beam dump embedded in the first part of the LEBT is mainly an aperture reduction of the cooled vacuum chamber. A negatively polarized ring located at the RFQ entrance acts as an electron barrier, and provides two functions: 1) Eliminating an electron flow from the LEBT into the RFQ which would provoke incorrect DCCT current measurements; 2) Inducing a better space charge neutralization near the RFQ entrance, helping beam focusing into the cavity. The pressure of a few 10^{-5} hPa gives a rise time for space charge neutralization of a few tens of microseconds.

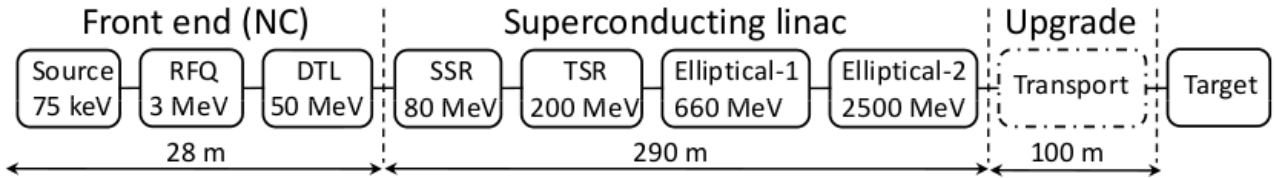


Figure 1: Block layout of the ESS linac. The space in the "Transport" section is reserved for a potential upgrade, in which additional cryomodules are installed to increase the beam power to 7.5 MW at a constant top energy of 2.5 GeV.

High beam intensity and low emittance growth are driving forces in the **RFQ** design, since it plays a significant role in determining the quality of the beam in the rest of the linac. The length of the bunching section exceeds 1 m in order to bunch the beam as adiabatically as possible. The conservative Kilpatrick value of 1.8 allows significant margin for a 4% duty cycle. The four vane structure has a variable voltage increasing from 66 kV to 100 kV, providing a high current limit. No resonant coupling gap is needed, thanks to the 4 m length. The resonator is mechanically divided into four segments, each with four tuners per quadrant. The **DTL** accelerates beam to 50 MeV, using a Linac4 based scheme in which three tanks are each fed by a single klystron (1.3 and 2.5 MW), for an accelerating gradient of more than 3 MV/m[5]. Post-couplers installed at every third drift tube stabilize the field profile against structural perturbations. The DTL has a very high shunt impedance thanks to the compact size of the drift tubes, which contain PMQs in an FFDD lattice. Single and Triple **Spoke Resonator** cavities are chosen to accelerate beam to 200 MeV because they are much less sensitive to mechanical perturbations than elliptical cavities, and because they provide large transit time factors in the β range from 0.3 to 0.5[6]. Installing SSRs with a FODO lattice just after the DTL enables cavities to be independently phased at relatively low energies, responding to the SNS experience that this is very useful for longitudinal acceptance tuning.

Table 2: Primary linac sub-system parameters.

System	T	Energy	Freq.	β	Length
	[K]	[MeV]	[MHz]	Geom.	[m]
Source	300	0.075	–	–	2.5
LEBT	300	–	–	–	1.1
RFQ	300	3	352.2	–	4.0
MEBT	300	–	352.2	–	1.1
DTL	300	50	352.2	–	19.2
SSR	4	80	352.2	0.35	23.3
TSR	4	200	352.2	0.50	48.8
Ellipt-1	2	660	704.4	0.65	61.7
Ellipt-2	2	2500	704.4	0.92	154.0

The electromagnetic design of the **elliptical cavities** originates in a single-cell cavity currently under testing for use in a BNL high-current ERL[7]. The design in Fig. 2 re-

duces the surface fields and relaxes tuning criteria[8]. **The power couplers** will deliver 1 MW of peak power with a 4% duty factor, causing the accelerating gradient to decrease in inverse proportion to the beam current. There is one coupler per cavity, with a single disk-type ceramic window to isolate the cavity vacuum. **Lorentz detuning** is dynamically compensated in order to constrain the resonant frequency of each cavity within the available bandwidth, maximizing the efficiency of energy transfer to the beam. Microphonics due to ambient acoustical noise also need to be considered. Stiffeners may be needed, to compensate for the inherent structural weakness of elliptical cavities. Detailed finite element analysis is underway to evaluate and optimize the closed loop system, including RF fill factor, cavity response, and dynamic tuning.

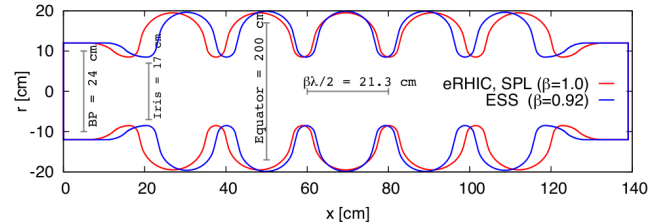


Figure 2: The five-cell 704 MHz cavity, showing the similarities between ESS, SPL and eRHIC structures.

Two families of elliptical cavities accelerate the beam to its final energy, using a **cryomodule** with 8 five-cell 704 MHz cavities that extends approximately 13 m. A continuous superconducting channel providing 2 K superfluid helium reduces cryogenic complexity and minimizes the number of external noise sources. Reducing the cryomodule length by shortening the transition section between cavities tends to reduce accelerating structure and civil engineering costs, but requires careful attention to the suppression of cross talk between neighboring cavities, and to efficient HOM damping and power extraction outside the cryogenic environment[8]. The transition section strongly damps the HOMs with a combination of multiple coaxial couplers and 80 K ferrites. The RF parameters of interest for the fundamental mode are listed in Tab. 3.

Cavity fabrication, testing and cryomodule assembly is complex and expensive, while quality control to assure the performance of ultra-clean cavity surfaces over hundreds of meters is challenging. Complex procedures need to be established in a horizontal cryomodule test stand, to

reliably reach 15 MV/m with a quality factor $Q_0 \geq 10^{10}$. A joint collaboration between ESS, BNL, CERN, Saclay and other institutes will develop a standard 704 MHz cryomodule to meet specific requirements of cavity-coupler performance, RF controls, cryogenics and operations.

Table 3: RF Parameters for 704 MHz five-cell cavities.

	ESS-1	ESS-2	eRHIC/SPL
Frequency [MHz]	704.4	704.4	703.8/704.4
β_{Geom} [v/c]	0.65	0.92	1.0
Cells/cavity	5	5	5
Cavities/module	8	8	6-8
E_p/E_a	3.52	2.58	2.34
H_p/E_a [$\frac{mT}{(MV/m)}$]	7.51	5.09	5.73
R/Q [Ω]	305	738	930
dF/dR [MHz/mm]	3.48	3.62	3.68
Cell coupling [%]	4.79	5.20	4.68

BEAM INSTRUMENTATION

The exact number of **Beam Loss Monitors**, and their strategic locations along the linac, are being optimized. They have multiple integration times with different abort limits to shut off the beam based on both small DC losses (causing activation at the ~ 1 W/m level) and loss spikes (causing problems with SC components). **Beam Current Monitors** use toroids that are integrated into the cryostats, limiting maintenance accessibility. **Beam Position Monitors** integrated into the cryostats near focusing quadrupoles enable stabilization schemes to center the beam in the aperture, reducing halo generation and minimizing beam losses[9]. Beam positions can also be measured using HOM damper signals. Candidate noninvasive **Beam Profile Monitor** technologies include Ionization Profile Monitors and beam scanners (Profilometers). IPMs, commonly used in rings[10], need a local pressure bump to enable single pass operation. Beam scanners pass a beam of ions or electrons at right angles through the main beam, and infer the profile from the deflection caused by the beam potential well[11]. Wire scanners can only be used at low intensities, and may distribute wire fragments in the vacuum system if they overheat and break[12]. Laser wire profile monitors unfortunately only work with H^- beams. **Quadrupole pick-ups** could be used to non-invasively measure the rms beam size, albeit not its distribution[13]. **A movable diagnostics plate** will be used for initial commissioning.

TARGET AND MODERATOR

A management structure is being put in place to minimize risks in building the long pulse target station, reflectors, moderators and neutron lines, and to complete the construction on time. Design optimization depends on: 1) Integrating diverse user requirements for all 22 instru-

ments; 2) Respecting ambitious but realistic safety objectives for operation, maintenance and de-commissioning; 3) Using robust nuclear industry standard qualifications for design and construction.

User requirements will be quantified as a set of neutron performance parameters for the instrument suite. The design process will explore several hundred combinations of all possible parameters, using a Design of Experiment methodology to allow the optimum combination of parameters to be determined in a finite amount of time. **Radiation release** guidelines will be calculated to limit the radiation doses to the population and the environment during normal operations and accident scenarios. Reference accident sequences will first be defined and documented in an Accident Analysis Specification, based on the actual design and on values in the Project Safety Guidelines. The most relevant parameters and assumptions will be documented in a Safety Analysis Data List, ensuring consistent conservative analysis. The PIE-PIT method will be used to identify paths along which radioactivity could be transported to the environment in an accident[14]. Defined accident sequences will then be analyzed, to verify that the design is robust and that releases would be well below acceptable levels. Equipment in the target – heavy metal liquid liquid circuits, beam windows, moderator mechanical supports, et cetera – may be exposed to moderate or major **structural damage** from irradiation, creep, fatigue, corrosion, pressure, or a combination. Their design, construction and operation – and manufacturers and sub-contractors – will respect qualified **nuclear industry design standards** RCC-MR (2007) and RCC-MX (2008), taking into account safety, reliability and cost requirements.

ACKNOWLEDGMENTS

Many thanks go to I. Ben-Zvi, P. Carlsson, J. Delayen, R. Garoby, F. Gerick, and A. Lombardi.

REFERENCES

- [1] H. Shober (ILL), Bilbao workshop presentation, 2009 <http://workshop2009.essbilbao.com/cas/wshopdoc/2.pdf>
- [2] "ESS Volume III Update: Technical report status", 2003.
- [3] L. Rybarczyk et al, Linac 2000.
- [4] P-Y. Beauvais et al, EPAC 2000.
- [5] F. Gerick et al, "RF structures for Linac4", PAC 2007.
- [6] K. Shepard et al, PRST-B 6, 080101 (2003).
- [7] R. Calaga, Ph.D. Thesis, Stony Brook University, 2006.
- [8] R. Calaga, C-AD Note, to be published, 2009.
- [9] "Conceptual Design of the SPL", CERN-2006-006.
- [10] A. Jansson et al, EPAC 2006.
- [11] P. Logatchov et al, RuPAC 2006.
- [12] S. Assadi, EPAC 2006.
- [13] A. Jansson, Ph.D. Thesis, 2001, CERN/PS 2001-014.
- [14] N. Taylor, "...Events for ITER Safety Analysis", SOFE 2003.